J Comp Physiol A (2014) 200:997–1013
DOI 10.1007/s00359-014-0950-y

ORIGINAL PAPER

Spectral sensitivity, luminous sensitivity, and temporal resolution of the visual systems in three sympatric temperate coastal shark species

Mieka Kalinoski · Amy Hirons · Andrij Horodysky · Richard Brill

Received: 30 January 2014 / Revised: 23 September 2014 / Accepted: 1 October 2014 / Published online: 16 October 2014

Abstract We used electroretinography (ERG) to determine spectral and luminous sensitivities, and the temporal resolution (flicker fusion frequency, FFF) in three sympatric (but phylogenetically distant) coastal shark species: *Carcharhinus plumbeus* (sandbar shark), *Mustelus canis* (smooth dogfish), and *Squalus acanthias* (spiny dogfish). Spectral sensitivities were similar (range ~400–600 nm, peak sensitivity ~470 nm), with a high likelihood of rod/cone dichromacy enhancing contrast discrimination. Spiny dogfish were significantly less light sensitive than the other species, whereas their FFF was ~19 Hz at maximum intensities; a value equal to that of sandbar shark and significantly above that of smooth dogfish (~9–12 Hz). This occurred even though experiments on spiny dogfish were conducted at 12 versus 25 °C and 20 °C for experiments on sandbar shark and smooth dogfish, respectively. Although spiny dogfish have a rod-dominated retina (rod:cone ratio 50:1), their visual system appears to have evolved for a relatively high temporal resolution (i.e., high FFF) through a short integration time, with the requisite concomitant reduction in luminous sensitivity. Our results suggest adaptive plasticity in the temporal resolution of elasmobranch visual systems which reflects the importance of the ability to track moving objects such as mates, predators, or prey.

Keywords Elasmobranch · Electroretinogram · Flicker fusion frequency · Temperature · Vision

Abbreviations

AIC	Akaike's information criterion
ERG	Electroretinography
FFF	Flicker fusion frequency
LLI	Log light intensity
MSP	Microspectrophotometry

Introduction

A true cosmopolitan class, elasmobranchs inhabit every aquatic realm, ranging from the darkness of the abyss, to brightly lit pelagic euphotic zones, to shallow murky coastal estuaries (Compango 1990; McFarland 1991; Klimley 2013). The visual demands under these conditions are drastically different (Litherland and Collin 2008). Although elasmobranchs employ an array of sensory modalities (Bleckmann and Hofmann 1999; Hodgson and Mathewson 1978), they generally show structural and physiological adaptations in their visual sense specific to their habitat or ecological requirements, demonstrating the importance of this sensory system (e.g., Hart et al. 2004; Schieber et al. 2012; Newman et al. 2013). Sensory biology, moreover, can be central to understanding predator–prey interactions, processes occurring between an organism and its environment, as well as predicting the effects

M. Kalinoski · A. Hirons
Oceanographic Center, Nova Southeastern University, 8000 N. Ocean Drive, Dania Beach, FL 33004, USA

A. Horodysky
Department of Marine and Environmental Science, Hampton University, 100 Queen Street, Hampton, VA 23668, USA

R. Brill
National Marine Fisheries Service, Northeast Fisheries Science Center, James J. Howard Marine Sciences Laboratory, 74 Magruder Road, Sandy Hook, Highlands, NJ 07732, USA

R. Brill (✉)
VIMS, PO Box 1346, Gloucester Point, VA 23062, USA
e-mail: rbrill@vims.edu

of changing environmental conditions (e.g., Sloman and Wilson 2006; Litherland et al. 2009; Healy et al. 2013). Insights into the adaptive responses of fishes' visual systems to their ecological niche can also help explain behavioral and life history characteristics, and vice versa (e.g., Levine and MacNichol 1979; Hueter 1991; Hueter et al. 2004; Wiessburg and Bowman 2005; McComb et al. 2013; Horodysky et al. 2008, 2010, 2013). Studies of visual adaptation have generally concentrated on comparing fishes from different photic environments (e.g., Douglas 2001; McComb et al. 2010; Litherland et al. 2009). Recent efforts have, however, also compared visual function in teleost species from similar visual environments or overlapping geographic areas, but with different ecologies or feeding strategies (e.g., Horodysky et al. 2008, 2010, 2013; McComb et al. 2013).

Electroretinography (ERG) has been used for over five decades to characterize visual function in elasmobranchs (e.g., Kobayashi 1962; Hamasaki et al. 1967; McComb et al. 2010; Bedore et al. 2013). Retinal responses to different wavelengths of monochromatic light produce spectral sensitivity curves and can indicate the capacity for color discrimination. Stimuli with incremental increases in light intensity produce an intensity–response curve (herein, referred to as V log I curve, where "V" refers to the voltage difference between the "a" and "b" waves of the ERG response to brief light flashes, and "I" refers to light intensity) (Evans et al. 1993). Shifts along the intensity axis in the V log I curve indicate either temporal (i.e., day vs. night) changes in retinal function due to retinomotor responses, or species-specific differences in luminous sensitivity (e.g., Horodysky et al. 2008, 2010, 2013; McComb et al. 2010). ERG employing a time-modulated light source can be used to measure the temporal properties of the retina. At low frequencies, retinal responses follow the modulated light signal in synchrony. But as the frequency of light flashes approaches the reciprocal of retinal integration time, the synchrony disappears and retinal responses resemble those produced by a continuous light source. The highest flash frequency producing synchronous retinal responses is generally referred to as the "flicker fusion frequency" (FFF) and provides a direct comparative measure of the temporal resolving power of different species (e.g., Horodysky et al. 2008, 2010, 2013; McComb et al. 2010).

ERG provides a comprehensive measure of the summed potentials of all of the cell types contained in the retina that are involved in optical detection (e.g., postsynaptic cells, pigment epithelium), not just the photoreceptor cells (Brown 1968; Armington 1974). The resultant data are, therefore, well-suited for comparative investigation of the functional properties of the visual systems in organisms relative to their specific photic environments, feeding strategies, etc. (e.g., Ali et al. 1978; Johnson et al. 2000; Frank 2003; Brill et al. 2008; Horodysky et al. 2008, 2010, 2013). Because ERG is an electrophysiological measurement, it requires access to live animals or at least recently isolated living retinal tissue (e.g., Fritsches et al. 2005); and this constrains the variety of elasmobranch species available for study. Data on FFF and luminous sensitivity (i.e., V log I curves) are available for a number of elasmobranchs (e.g., Kobayashi 1962; Hamasaki and Bridges 1965; O'Gower and Mathewson 1967; Cohen et al. 1977; Bullock et al. 1991; Gačić et al. 2007a, b; Bedore et al. 2013). But these two parameters have received less attention than spectral sensitivity (i.e., the presence or absence of various visual pigments and their match or mismatch to the photic environment) (e.g., Hart et al. 2004, 2011; Gačić et al. 2007b; Bedore et al. 2013) and anatomical adaptations relevant to spatial resolving power or other parameters (e.g., retinal topography, rod-to-cone ratios, receptor cell convergence on bipolar cells, etc.). This situation occurs because, in contrast to FFF and luminous sensitivity which must be measured via ERG, the other parameters can be investigated with preserved specimens using microspectrophotometry (MSP) or standard anatomical procedures (e.g., Litherland and Collin 2008; Lisney et al. 2012; Schieber et al. 2012; Newman et al. 2013).

To allow visual function at low light levels, animals employ both spatial and temporal summation within the retina (Warrant 1999, 2004). Although they enhance retinal sensitivity, both require inevitable tradeoffs. Spatial summation reduces visual acuity, and temporal summation comes with the cost of reduced temporal resolution (i.e., lower FFF) and, therefore, a blurring of the details of fast moving objects, or the inability to detect them at all (Warrant 1999, 2004; Frank 1999, 2000). The latter situation is roughly analogous to effects of slow shutter speeds in a camera (Lythgoe 1979). The converse is also true, however. In the absence of elevated retinal temperatures, high temporal resolution (i.e., a high FFF) necessarily must be accompanied by a reduced luminous sensitivity (i.e., a rightward shift in the retinal V log I curve).

The ability of sharks (and organisms in general) to detect, track, and capture mobile prey, to avoid predators and objects, and to recognize conspecifics depends on the luminous sensitivity and temporal resolution, as well as the spectral sensitivity of their visual systems and its match–mismatch to background space-light (e.g., Lythgoe 1978; Lythgoe and Partridge 1991; Healy et al. 2013). All three are, therefore, relevant to understanding species-specific visual ecology and the evolutionary plasticity of visual function (e.g., Warrant 1999; Marshall et al. 2003). The aim of our study was, therefore, to determine the extent of similarities and differences in

spectral sensitivity, luminous sensitivity (V log I curves), and temporal resolution (FFF) among three coastal shark species: *Carcharhinus plumbeus* (sandbar shark), *Mustelus canis* (smooth dogfish, also commonly called dusky smooth hound), and *Squalus acanthias* (spiny dogfish). Because their geographic ranges and prey species overlap (described more fully below), these three species present the opportunity to compare three ecologically similar, but phylogenetically distant, elasmobranchs (Compagno 1984a, b, 1990, 2003; Klimley 2013). We are thus attempting to tease apart the relative importance of environment and phylogeny on shaping visual function in elasmobranchs. We used ERG as it provides data directly comparable to other published work, including data on teleost fishes from the same coastal environment (Horodysky et al. 2008, 2010, 2013).

Sandbar shark, smooth dogfish, and spiny dogfish have sympatric distributions over the continental shelf and within the tidal estuaries of the mid-Atlantic and northeast US east coast. They do not, however, generally occupy the same areas at the same time of year because of differences in their thermal ecology (Collette and Klein-MacPhee 2002; Grubbs and Musick 2007; Grubbs et al. 2007; Conrath and Musick 2008). Sandbar shark (Superorder Galeomorphi, Order Carcharhiniformes, Family Carcharhinidae) is a ubiquitous demersal species with near-circumglobal distribution in warm temperate and tropical coastal and adjacent offshore waters exclusive of the eastern Pacific Ocean (Compagno 1984b; McCandless et al. 2007; Conrath and Musick 2008; Able and Fahay 2010). On the U.S. east coast, this species migrates north during the summer months with females giving birth to pups in mid-Atlantic estuaries (e.g., Delaware Bay and Chesapeake Bay). The pups overwinter in areas offshore of North Carolina and return to the same estuaries during the summer months for up to 5 years (Collette and Klein-MacPhee 2002; Grubbs et al. 2007; Able and Fahay 2010). In estuarine nursery grounds, pups feed primarily on blue crab (*Callinectes sapidus*), mantis shrimp (*Squilla empusa*), other crustaceans, as well as small fishes; on continental shelf areas, their diet consists primarily of small fishes (Stillwell and Kohler 1993; Collette and Klein-MacPhee 2002; Able and Fahay 2010). Smooth dogfish (Superorder Galeomorphi, Order Carcharhiniformes, Family Triakidae) is one of the most abundant inshore sharks along the east coast of the United States, seasonally ranging from Massachusetts (south of Cape Cod) to Florida (Rountree and Able 1996; Collette and Klein-MacPhee 2002; Conrath and Musick 2002). Like sandbar shark, smooth dogfish pup in U.S. east coast estuaries (e.g., Delaware Bay and Chesapeake Bay) during the summer months with the pups overwintering in offshore areas from North Carolina to the Gulf of Mexico (Able and Fahay 2010). Smooth dogfish feed primarily on decapod crustaceans, but a significant portion of the diet also consists of squids, bivalves, and gastropods (Gelsleichter et al. 1999; Rountree and Able 1996). Spiny dogfish (Superorder Squalomorphi, Order Squaliformes, Family Squalidae) are usually found in aggregations that typically number in the hundreds (Collette and Klein-MacPhee 2002). They forage in "packs" attacking schools of fishes which form the majority of their diet, the second largest component being mollusks (McMillan and Morse 1999; Collette and Klein-MacPhee 2002). Spiny dogfish occur in the temperate and boreal waters of the Atlantic Ocean. During the summer months in the northwest Atlantic, they occur primarily in the Gulf of Maine (i.e., north of Cape Cod, Massachusetts where they are the most abundant shark species); and during the winter months, they occur as far south as North Carolina. Their distribution reflects preferred and upper limiting temperature (6–8 °C and 15 °C, respectively) (Collette and Klein-MacPhee 2002).

Materials and methods

Juvenile sandbar sharks and smooth dogfish were captured between May and June from tidal estuaries in the northwest Atlantic Ocean along the eastern shore of Virginia. They were transported to the holding facilities at the Virginia Institute of Marine Science, Eastern Shore Laboratory (Wachapreague, VA, USA). Sandbar sharks were kept in an outdoor circular fiberglass tank (~8 m in diameter and 2 m deep) that was shaded with a black mesh cloth awning to protect the animals from direct sunlight. It was supplied with filtered seawater from the adjacent tidal lagoon; water temperature was not controlled and reached a maximum of 26 °C. Smooth dogfish were maintained in indoor tanks supplied with recirculated seawater maintained at 20 ± 1 °C. The indoor tanks likewise experienced a natural light: dark cycle. Sandbar sharks and smooth dogfish were housed for a maximum of 8 weeks before use in an experiment. Spiny dogfish were captured offshore of southeastern Massachusetts (northwest Atlantic Ocean) in September and October using conventional sport fishing gear. They were transported to the holding facilities at the University of Massachusetts Dartmouth—School for Marine Science and Technology (New Bedford, MA, USA) and held in an indoor circular fiberglass tank (~4,000 L) supplied with filtered and aerated seawater (10–14 °C). The tank was illuminated with overhead fluorescent lights, but fish were exposed to an approximately normal photoperiod (11 h light, 13 h dark). Individuals were in captivity less than 4 weeks before use in an experiment.

Immediately prior to use in an experiment, fish were injected (IV) with ketamine hydrochloride (30 mg kg^{-1},

Butler Animal Health, Middletown, PA, USA), an effective anesthetic in fishes (Ross and Ross 1999), followed by an IV injection of the neuromuscular blocking drug pancuronium bromide (1 mg kg^{-1}, Sigma-Aldrich Inc., St. Louis, MO, USA). The latter was used to minimize electrical interference from muscular noise. Additional doses of the drugs were administered during the course of the experiment on an as-needed basis. After initial drug injections, each shark was transported to a light restricted room and placed on a submerged cloth sling suspended within a rectangular experimental plexiglass tank. Individuals were positioned such that only the left eye and a small portion of the head were above the waterline, and were artificially ventilated with aerated seawater via a hose attached to a small pump. Fish were also covered with a wet towel, exclusive of the head and gill slits. The temperature of the seawater in the experimental tank was maintained at 25 °C (sandbar shark), 20 °C (smooth dogfish), or 12–13 °C (spiny dogfish). Additional experiments with smooth dogfish were also conducted at 12 °C specifically to test the effects of temperature on FFF. In all cases, subjects were dark adapted for at least 1 h prior to the start of data recording which was sufficient to allow maximal pupil dilation (Kajiura and Tallack 2009; Kajiura 2010). Sharks were euthanized at the completion of an experiment by a massive overdose (300 mg kg^{-1}, ~10× the anesthetic dose) of sodium pentobarbital (Schering-Plough Animal Health, Union, NJ, USA) injected via the caudal vein.

Spectrophotometry of the ocular media

To assess the transmission properties of the ocular media, the cornea, lens, and vitreous humor were dissected from freshly euthanized sharks and tested individually using a Shimadzu BioSpec-1601 spectrophotometer (Shimadzu Scientific Instruments, Columbia, MD), accompanying software, and UV transmitting cuvettes. Corneas and lens were submerged in cuvettes filled with elasmobranch Ringer's solution (280 mM NaCl, 12 mM KCl, 10 mM $CaCl_2{\cdot}2H_20$, 4.5 mM $NaHCO_3$, 5 mM $MgCl{\cdot}6H_20$, 0.5 mM NaH_2PO_4, 360 mM Urea, 90 mM TMAO, pH 7.8) and positioned to ensure the light beam passed through the tissue. Samples of vitreous humor were placed directly in the cuvettes. Transmission of the isolated ocular media was measured in 5 nm steps over wavelengths from 250 to 750 nm. The data were subsequently smoothed using a five-point moving average.

Electroretinography

Whole-animal corneal ERG responses to light stimuli were recorded from live animals (during both day and night to account for natural circadian rhythms) using Teflon-coated silver–silver chloride electrodes. The active (i.e., recording) electrode was placed on the corneal surface and the reference electrode positioned subdermally on the top of the head approximately 2 cm from the eyecup. Electrode placements, as well as any further modifications to the experimental setup, were conducted under a dim red LED light source (peak wavelength of 660 nm) that was well beyond the visual capabilities of elasmobranch species (Hart et al. 2004).

Signal amplification and filtering, data recording, processing, and data analysis techniques were as described previously (Brill et al. 2008; Horodysky et al. 2008). In brief, retinal response recordings and stimulus presentation were controlled with a multifunction data acquisition card (DAQ, model 6024E, National Instruments, Austin, TX USA) using custom-designed software (originally developed by Eric Warrant, University of Lund, Lund, Sweden) written in LabVIEW graphical programming system (National Instruments, Austin, TX, USA). Retinal function in the dark-adapted state was assessed using four separate *modus operandi*: (1) spectral sensitivity, (2) luminous sensitivity (V log I response), (3) FFF vs. intensity, and (4) FFF vs. contrast.

Spectral sensitivity experiments used procedures described in Brill et al. (2008) and Horodysky et al. (2008) to assess the ability of the visual systems of the three shark species to respond to monochromatic light stimuli (50 % bandwidth = 5 nm) ranging from UV (300 nm) to the far red (650 nm) in 10 nm steps. Monochromatic light flashes of near equal quantal energy were produced using a xenon fiber-optic light source (Y1603, ILC Technology, Sunnydale, CA, USA), a monochromator (model CM110, CVI Laser Spectral Products, Albuquerque, NM, USA), and two filter wheel assemblies (model AB301, CVI Laser Spectral Products, Albuquerque, NM, USA) equipped with quartz neutral density filters which together allowed the attenuation of light from 0 to 5 log units in 0.2 log unit steps. The LabVIEW program controlled the monochromator and filter wheel assemblies via serial interfaces, and a Uniblitz electronic shutter (model LS6, Vincent Associates, Rochester, NY, USA) using the digital output of the DAQ card. Five single 40-ms flashes at each experimental wavelength were presented through a 1 cm diameter light guide (with quartz ends) placed within approximately 5 cm of a subject's eye. Each flash was followed by 5 s of darkness. The amplitudes of the responses to individual flashes were averaged to form raw spectral response curves for each individual. A spectral V log I response curve was also obtained for each subject at the wavelength (λ_{max}) that generated the maximum response (V_{max}) to facilitate the subsequent calculation of the subject's spectral sensitivity curve at equal quantal light intensities as described by Coates

et al. (2006). Spectral *V* log *I* response experiments exposed the subject to five individual monochromatic flashes of 200 ms duration at each intensity, separated by 5 s of darkness, increasing in 0.2 log unit increments over five orders of magnitude. Spectral response voltages were transformed to spectral sensitivities for each subject by converting the former to equivalent intensities and expressing them on a percentage scale (100 % indicating maximum sensitivity) using Eq. (1):

$$S = 100 \times 10^{-|I\max - I_n|} \quad (1)$$

where S = spectral sensitivity, I_{max} = intensity at maximum response voltage, I_n = intensity at response voltage n.

Finally, the spectral sensitivity curves were normalized with the maximal response set as 100 %. The final spectral sensitivity curves for each species were constructed by taking the mean for all individuals, with the mean data subsequently re-scaled from 0 to 100 %.

Protocols to measure luminous sensitivity (*V* log *I* curves) employed a custom-built single LED light source (working range ~1 to 1 × 10^4 cd m^{-2}) with an attached diffuser and collimating lens to produce an even illumination field. Lamp output was calibrated with a research radiometer (model IL 1700, International Light, Inc., Newburyport, MA, USA). The angle and distance of light source relative to the retina remained steady throughout each experiment and bathed the entire eye in light. The analog output of the DAQ card controlled the absolute brightness of the lamp and combinations of 1.0 and 2.0 log unit neutral density filters (Kodak Optical Products, Rochester, NY, USA) were used as needed to adjust further the range of light intensities. *V* log *I* data were obtained using 0.2 log unit steps from sub-threshold to light levels above that needed to define the *V* log *I* curve (Evans et al. 1993, Severns and Johnson 1993). Retinal responses were recorded from a train of five 200-ms flashes at each intensity step, each separated by 200-ms rest periods, but only the last flash of each stimulus train was used for analysis. This process was repeated five times and the data averaged. The amplitude of the response (in μV) was taken as the difference between the minimum value of the negative-going a-wave (when present) and the maximum value of the positive-going b-wave, as is standard procedure for describing the relationship of retinal responses and stimulus intensity (i.e., *V* log *I* curves) (Evans et al. 1993).

FFF experiments used the white light LED source described above and followed procedures described previously (Fritsches et al. 2005; Brill et al. 2008; Horodysky et al. 2008). For each individual, FFF experiments were performed at intervals from very dim light to levels at or slightly above those needed to produce maximum responses recorded during the *V* log *I* experiments. At each light level, 5-s trains of sinusoidal light stimuli

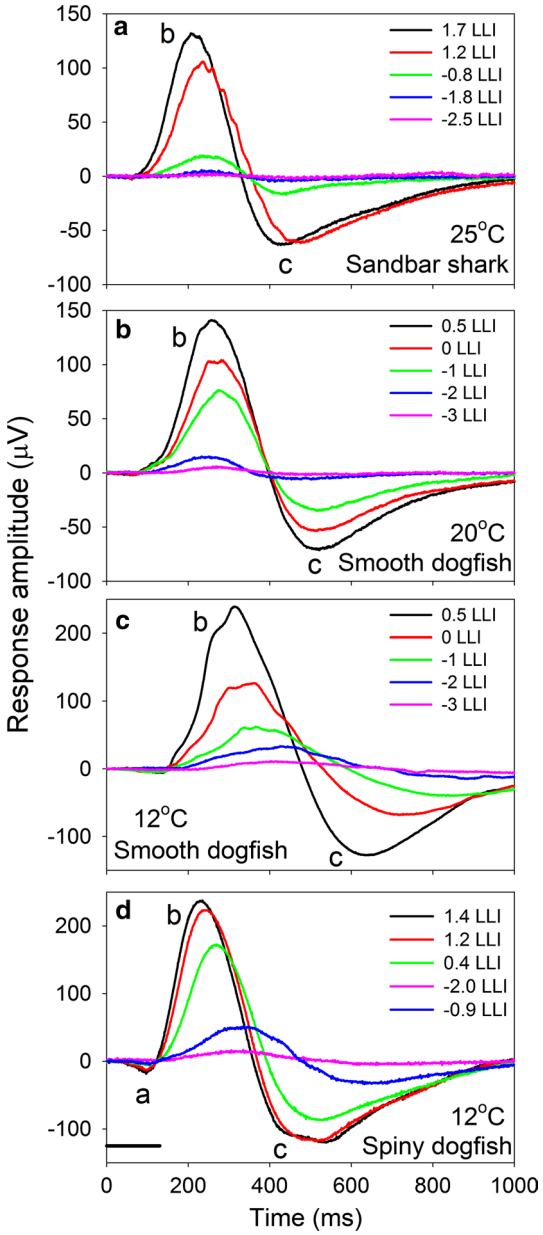

Fig. 1 Representative ERG responses from sandbar shark 25 °C (**a**), smooth dogfish at 20 °C (**b**), smooth dogfish at 12 °C (**c**), and spiny dogfish 12 °C (**d**) to white light flashes of fixed duration (130 ms) and various intensities (expressed as log units of cd m^{-2}). *b*- and *c*-waves were present in all three species, and their amplitudes increased with increasing light intensities. In contrast, *a*-waves were clearly present only at the two highest light intensities in spiny dogfish. The onset and duration of the white light stimulus are shown by the *solid line in* **d**

(frequency range: 1 Hz [0 log units] to 25.1 Hz [1.4 log units]) were presented in 0.2 log unit frequency steps, repeated five times at each frequency with a 5-s interval between repetitions, and responses averaged. Power spectrums were calculated through Fourier transformation using a custom-designed LabVIEW program (originally developed by Eric Warrant, University of Lund, Lund,

Sweden). Critical FFF was taken as the point where the power at the stimulus frequency dropped below the power of the noise at the same frequency. In addition, FFF was determined at five different contrasts (100, 50, 10, 5 and 1 %; i.e., where depth of the stimulus was modulated), with contrast calculated as:

$$\text{contrast} = \left[\left(I_{\max} - I_{\min}\right) / I_{\max}\right] \times 100 \quad (2)$$

where $I_{\max}$ = maximum intensity, $I_{\min}$ = minimum intensity.

Two light intensities were tested at each contrast step, one equal to 25 % of saturating brightness levels (which varied between individual sharks) and one at 0.8, 0.5, or 1.4 LLI which were approximately the intensities required to produce the maximum responses in the V log I experiments in sandbar sharks, smooth dogfish and spiny dogfish, respectively.

For purely illustrative purposes to show their specific shape and the presence or absence of a-, b- and c-waves (Fig. 1), we also recorded ERG responses from sandbar shark, smooth dogfish (at two temperatures), and spiny dogfish to single white light flashes (130 ms duration) produced by the white light LED source and combinations of neutral density filters. Five single flashes, 10 s apart, were presented at each of five light intensities and the responses at each intensity averaged.

Statistical procedures

The Naka–Rushton equation was fitted to the response data (V_I) and stimulus intensity (I, in cd m^{-2}) for each individual (during the day and night):

$$V_I = \left(V_{\max} I^n\right) / \left(I^n + K^n\right) \quad (3)$$

where $V_{\max}$ = asymptotic response amplitude, n = slope of the linear portion of the V log I curve, K = stimulus irradiance eliciting a response equal to one half $V_{\max}$, using OriginPro 9.1.0 (OriginLab Corp., Northampton, MA, USA). Because $V_{\max}$ values were not accurately predicted in every instance, the K values were also not predicted. We, therefore, took the 50 % response point from the predicted values of V_I equal to one half of the $V_{\max}$, with the latter taken as the initial plateau of the response prior to its dip in amplitude that sometimes preceded its increase to a second limb (Severns and Johnson 1993). The 50 % response values were subsequently averaged across species and condition (i.e., day vs. night). The normalized V log I curves of individuals of each species were also used to construct mean (±standard error of the mean, SEM) V log I curves. For subsequent plotting, the resultant normalized voltage data were subsequently re-scaled to 0–100 %.

Statistical analyses were performed using Sigma Plot for Windows version 11.2 (Systat Software Inc., San Jose, CA, USA). Data from experiments to determine luminous sensitivity (50 % V log I) were analyzed using a two-way ANOVA (factors: species, photoperiod, and irradiance level) with pairwise multiple comparisons. Temporal responses (i.e., FFFs) were analyzed using two-way repeated measures ANOVA within species (factors: photoperiod and irradiance level), and with a one-way repeated measures ANOVA to compare flicker fusion frequencies between species at light intensities required to produce the 25 and 100 % response points in the V log I curves.

To form hypotheses regarding the number and spectral absorption of pigments potentially contributing to spectral ERG responses, we fitted the SSH (Stavenga et al. 1993) and GFRKD (Govardovskii et al. 2000) vitamin A1 rhodopsin absorbance templates separately to the spectral sensitivity data following procedures described by Horodysky et al. (2008, 2010). We considered scenarios with one or two alpha (α) band rhodopsins, the latter with and without the presence of β bands on the shorter wavelength pigment. For a given species, condition and template, models of summed curves were created by adding the products of pigment-specific templates and their respective weighting factors. Estimates of the unknown model parameters ($\lambda_{\max}$ values and their respective weighting proportions) were derived by fitting the summed curves to the ERG data using maximum likelihood.

For each species, we objectively selected the appropriate template (SSH or GFRKD) and number of contributing pigments using an Information Theoretic approach (Burnham and Anderson 2002) following Akaike's Information Criterion (AIC):

$$\text{AIC} = -2\ln(\hat{L}) + 2p \quad (4)$$

where AIC Akaike's Information Criterion, $\hat{L}$ the estimated value of the likelihood function at its maximum, p number of estimated parameters.

This technique balances model complexity and parsimony in selecting the conditions that best explain the underlying data. Parameter optimization, template fitting, and model selection were conducted using the software package R, version 2.12.1 (R Development Core Team 2008).

Results

The size ranges of the fishes used in our experiments are given in Table 1. While all three species displayed clear b- and c-wave responses (Fig. 1), as do other shark species (e.g., McComb et al. 2010), only spiny dogfish showed a clearly discernable a-wave, and generally only at the two highest light intensities employed.

Table 1 Fork lengths and body masses of the three shark species investigated

Species	Fork length (cm)	Body mass (kg)
Sandbar shark	63–77	2.3–4.7
Smooth dogfish	53–91	0.45–1.57
Spiny dogfish	62–72	1.2–2.0

Spectral sensitivity

Sandbar sharks showed ERG responses to monochromatic light flashes over the spectral range of ~320–600 nm, albeit with a clear increase in sensitivity above 420 nm, and two peaks in maximal sensitivity spanning the blue to green-yellow region of the spectrum (480 and 520 nm, Fig. 2). Smooth dogfish spectral responses were similar, spanning the range of ~340–590 nm, with a clear increase in sensitivity above 410 nm; but with only an apparent single peak in maximal sensitivity at 470 nm (Fig. 2). As with the other two species, the responses of spiny dogfish increased sharply at wavelengths above 390 nm, although they were clearly less responsive to wavelengths below this than were sandbar shark. Spiny dogfish exhibited only an apparent single peak in spectral sensitivity (at 470 nm) during the day, which shifted to a slightly higher wavelength (480 nm) at night. They also showed a clear shift in the lower half of the spectral curve (i.e., below ~500 nm) to shorter wavelengths at night. There were no substantial changes in spectral sensitivity between day and night recordings in sandbar shark or smooth dogfish (Fig. 2).

To formulate hypotheses on the number of pigments present, the day ERG data were fitted to the SSH (Stavenga et al. 1993) and GFRKD (Govardovskii et al. 2000) vitamin A_1 rhodopsin absorbance templates. Three possible conditions were considered: (1) one to three α band rhodopsins, (2) one to three α band rhodopsins with a single beta (β) band, and (3) one to three α band rhodopsins with multiple β bands. The condition, template, and models of the summed curves were created by adding the products of pigment-specific templates and their respective weighting factors, derived by fitting the summed curves to the ERG data using maximum likelihood (Horodysky et al. 2008). The correct template and number of contributing pigments were chosen based on an Information Theoretic approach following Akaike's Information Criterion (AIC) (Table 2). AIC is an estimate of the maximum likelihood of one of these conditions, given the fixed estimated parameters. The AIC value provides a quantitative measure to determine the estimates of the rhodopsin parameters based on the data (Horodysky et al. 2008).

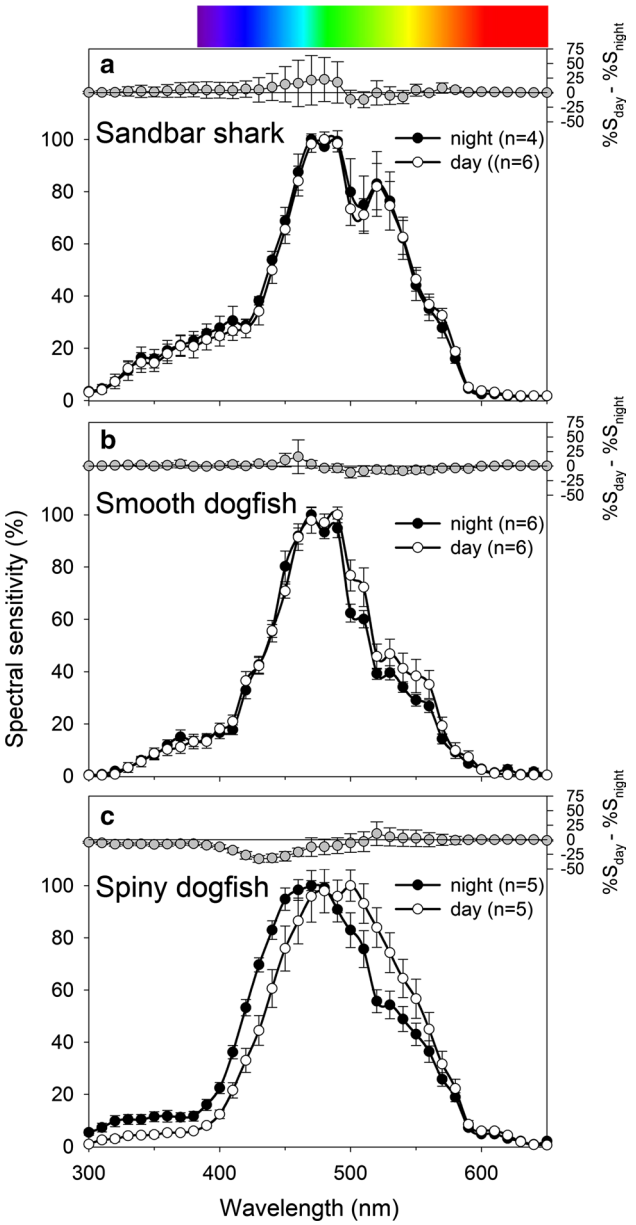

Fig. 2 Mean (±SEM) spectral sensitivity curves calculated from the retinal responses for wavelengths of 300–700 nm. *Open circles* show results from day experiments and *filled circles* results from night experiments. The *top panels* (*gray circles, right axes*) are the mean diel differences in spectral sensitivity calculated by subtracting the retinal responses during the day from those recorded at night for each individual. The *vertical bars* are ±95 % confidence intervals, calculated as 1.96 × SEM. Significant diel differences are indicated when confidence intervals do not encompass zero. The *color bar at the top of the figure* shows the human visual spectrum relative to wavelength

The data from sandbar shark were equally well fit by the SSH rhodopsin template with two α band rhodopsins with a single β band, and the SSH and GFRKD rhodopsin templates with three α band rhodopsins (Table 2). Given that the preponderance of evidence is for cone monochromacy

Table 2 Parameter estimates and model rankings of SSH (Stavenga et al. 1993) and GFRKD (Govardovskii et al. 2000) vitamin A1 rhodopsin templates fitted to the spectral ERG data via maximum likelihood

Species	Rhodopsin[a]	Template	$\lambda_{max,1}$[b]	$\lambda_{max,2}$	$\lambda_{max,3}$	$-\log(L)$[c]	P[d]	AIC	ΔAIC
Sandbar	1	GFRKD	496	–	–	−28.1	2	−52.3	30
shark		SSH	496	–	–	−30.9	2	−57.7	24.6
	2	GFRKD	474	521	–	−36.1	5	−62.2	20.1
		SSH	478	526	–	−39.2	5	−68.5	13.7
	2B	GFRKD	478	521	–	−45.8	6	−79.7	2.6
		SSH	**481**	**528**	**–**	**−46.6**	**6**	**−81.1**	**1.2**
	3	**GFRKD**	**366**	**478**	**524**	**−48.2**	**7**	**−82.3**	**0**
		SSH	357	481	529	**−47.2**	**7**	**−80.4**	**1.9**
Smooth	1	GFRKD	485	–	–	−39.6	2	−75.2	12.9
dogfish		SSH	486	–	–	−40.7	2	−77.3	10.8
	2	**GFRKD**	**477**	**538**	**–**	**−48.4**	**5**	**−86.8**	**1.3**
		SSH	**478**	**544**	**–**	**−49.1**	**5**	**−88.1**	**0**
	2B	GFRKD	479	541	–	−48.3	6	−84.6	3.5
		SSH	479	543	–	−48.1	6	−84.2	3.9
	3	**GFRKD**	**355**	**477**	**538**	**−50.3**	**7**	**−86.5**	**1.6**
		SSH	342	478	543	−49.2	7	−84.5	3.6
Spiny	1	GFRKD	498	**–**	**–**	−41.6	2	−79.1	102.3
dogfish		SSH	498	–	–	−41.3	2	−78.7	100.2
	2	**GFRKD**	**472**	**520**	**–**	**−78.9**	**5**	**−147.9**	**0**
		SSH	476	523	–	−70.4	5	−130.9	17
	2B	GFRKD	488	543	–	−58.5	6	−105.1	42.8
		SSH	489	531	–	−49.6	6	−87.2	**60.7**
	3	**GFRKD**	**334**	**472**	**521**	**−80.3**	**7**	**−146.7**	**1.2**
		SSH	312	476	523	−70.5	7	−127	20.9

Bold type indicates the best supported pigment and template scenarios based on Akaike's information criterion (AIC) values (lower is better)

ΔAIC (AIC_{lowest}−AIC) values <2 are statistically indistinguishable and have equal support; in those instances, we selected the most parsimonious explanation

[a] "1" = single rhodopsin, "2" = two rhodopsins, "2B" = two rhodopsins with a β band on the long wavelength pigment, "3" = three rhodopsins

[b] The subscripts "1", "2", and "3" refer to the wave lengths of maximum absorption of pigments 1, 2, and 3

[c] L is the value of the likelihood function

[d] "P" is the number of parameters in a model

in sharks (Hart et al. 2011), we conclude that the former is more likely. We also presume the long and short A_1 rhodopsin α band photo pigments (λ_{max} 541 nm and 481 nm, respectively) represent rod and cone cells, and that the β band (maximally absorption at 351 nm) resides on longer wavelength pigment (Fig. 3).

The data from smooth dogfish were best fit by the SSH rhodopsin template with two α band rhodopsins. It, therefore, appears that smooth dogfish likewise have both a shorter wavelength A_1 rhodopsin α band photo pigment, (λ_{max} 478 nm) and a longer wavelength pigment (λ_{max} 544 nm). Stell and Witkovsky (1973) reported that the retina of smooth dogfish contains only one type of visual pigment. Our spectral response curves suggest, however, that at least two photopigments are present. Given the very high rod-to-cone ratio (100:1) reported in smooth dogfish (Stell and Witkovsky 1973), we assume that the predominate shorter wavelength pigment is most likely within the rod photoreceptors, with the contribution of the longer wavelength pigment in the less numerous cone cells creating the slight shoulder seen in the spectral sensitivity curve between 520 and 560 nm (Fig. 3).

The data from spiny dogfish were best fit by the GFRKD rhodopsin template with two α band rhodopsins. Therefore, it appears that spiny dogfish likewise have both a shorter wavelength A_1 rhodopsin α band photo pigment (λ_{max} 472 nm), and a longer wavelength pigment (λ_{max} 520 nm). But unlike sandbar sharks, there is no evidence of a β band. Unlike either of the other two species, the longer wavelength pigment predominates, but in this case only slightly so (Fig. 3).

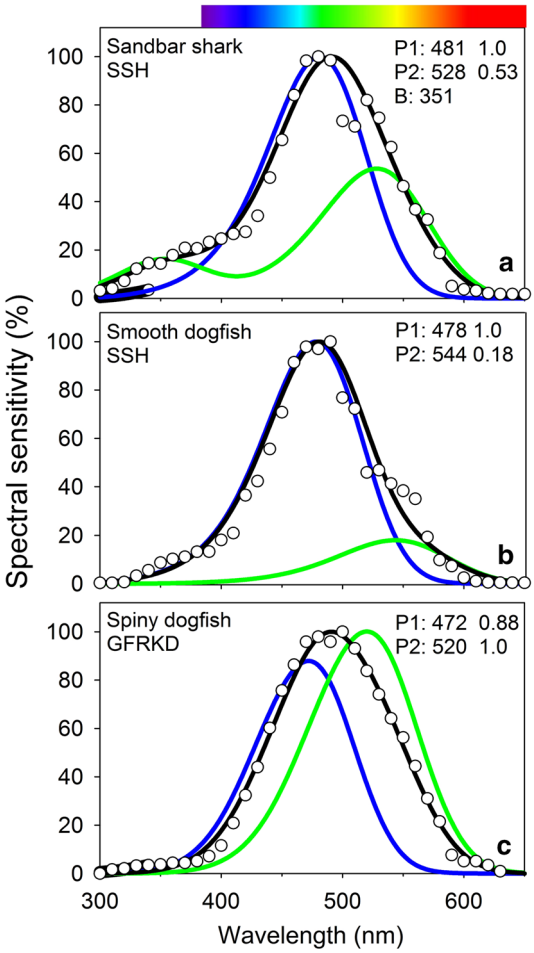

Fig. 3 SSH (Stavenga et al. 1993) and GFRKD (Govardovskii et al. 2000) vitamin A1 templates fitted to spectral sensitivity data for sandbar shark (**a**), smooth dogfish (**b**), and spiny dogfish (**c**) by maximum likelihood using the best fitting models from Table 2 and following procedures described by Horodysky et al. (2008, 2010). Values to the right are estimated λ_{max}, pigment-specific weight values, and absorption maximum of the β band (sandbar shark only) estimated by the model. P1 (*blue lines*) are the short wavelength pigments, P2 (*green lines*) are the longer wavelength pigments. *Black lines* show additive curves developed by summing the product of each curve multiplied by the estimated weighting factor. The *open circles* are mean values from Fig. 2. The *color bar at the top of the figure* shows the human visual spectrum relative to wavelength

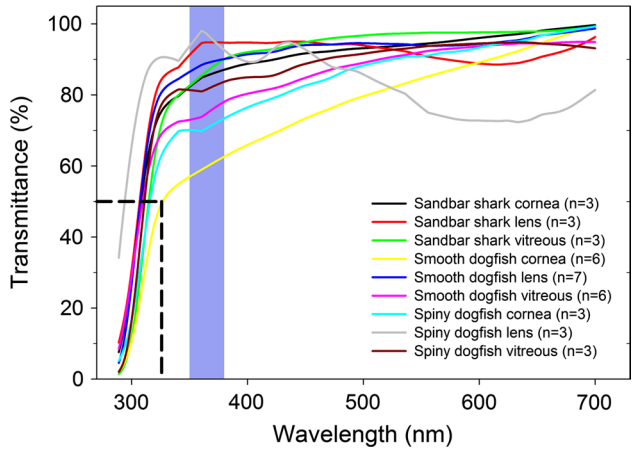

Fig. 4 Relative spectral transmission of the corneas, vitreous humors, and lenses of sandbar shark, smooth dogfish, and spiny dogfish. UV-A wavelengths (350–380 nm) are indicated by the *shaded area*. The *dashed lines* show the highest wavelength by which transmission is reduced by 50 % (λ_{T50})

Spectrophotometry of the ocular media

Spectrophotometric examination of the transmission ocular media revealed that wavelengths in the UV-A range (350–380 nm) were transmitted through the cornea, lens, and vitreous of all three shark species (Fig. 4). It is common practice to describe the spectral transmission of light passing through elements of the ocular media by the wavelength by which transmission is reduced to 50 % (λ_{T50}, e.g., Thorpe et al. 1993; Siebeck and Marshall 2001; Losey et al. 2003; Litherland et al. 2009). The λ_{T50} of all three components from all three species is equal to or below 326 nm, which is well into the UV range.

V log *I* response curves

V log *I* response curves of all three shark species (Fig. 5) did not have the strict sigmoidal shape as is predicted for photoreceptor cell function based on the Naka–Rushton model (Naka and Rushton 1966). Rather, responses increased monotonically with stimulus intensity to maximum amplitudes (V_{max}). They then either remained stable with increases in light intensity over a limited range (sandbar shark) presumably due to photoreceptor saturation, or immediately decreased (smooth and spiny dogfish) presumably due to a lack of pigment regeneration. Based on the 50 % points of the normalized *V* log *I* curves, we found significant differences in luminous sensitivity between species (two-way ANOVA, $F = 26.6$, $P < 0.001$), but no significant day versus night differences ($F = 0.16$, $P = 0.69$). Isolating the effects of species showed that spiny dogfish had a significantly ($P < 0.001$) lower mean luminous sensitivity [i.e., a higher mean (±SEM) log light intensity (LLI) (based on cd m^{-2}) at the 50 % response point: 0.26 ± 0.8 s^{-1}] compared to those of sandbar shark and smooth dogfish [mean (±SEM) LLI (based on cd m^{-2}) at the 50 % response points: -0.49 ± 0.10 and -0.42 ± 0.07, respectively]. No interaction terms (i.e., species × day vs. night) were significant.

Flicker fusion frequency

Based on repeated measures ANOVA, there were no significant day versus night differences in FFF and the data were,

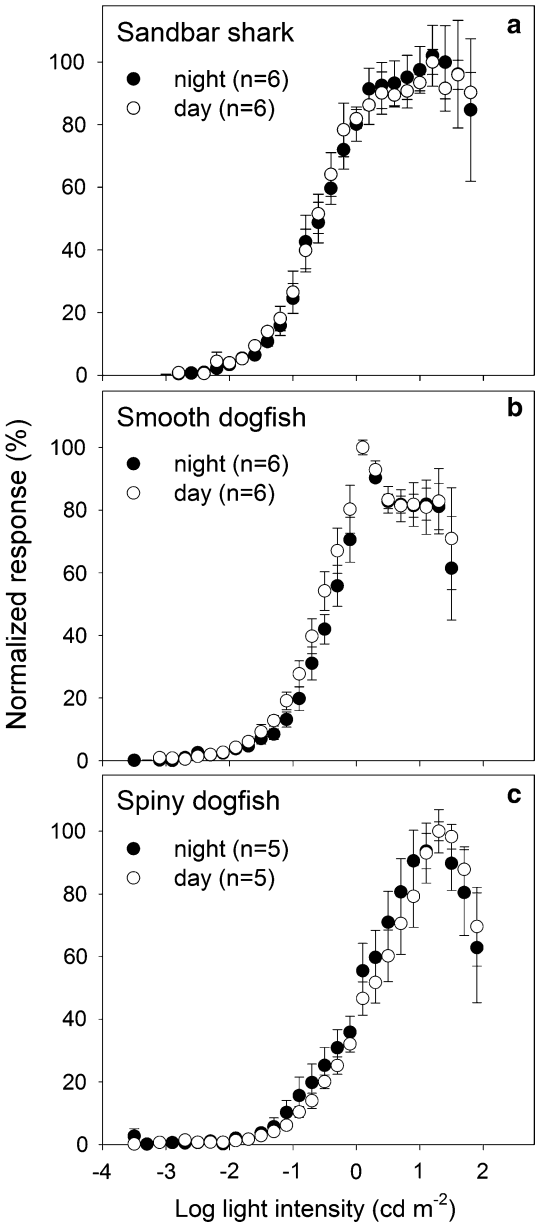

Fig. 5 Mean (±SEM) V log I (i.e., intensity–response) curves for sandbar shark (**a**), smooth dogfish (**b**), and spiny dogfish (**c**), where "*V*" refers to the voltage difference between the a- and b-waves of the ERG response to 200-ms flashes of white light, and "*I*" refers to light intensity (in cd m^{-2}). *Open symbols* are data from day experiments and *filled symbols* data from night experiments. Response values have been normalized from 0 to 100 %

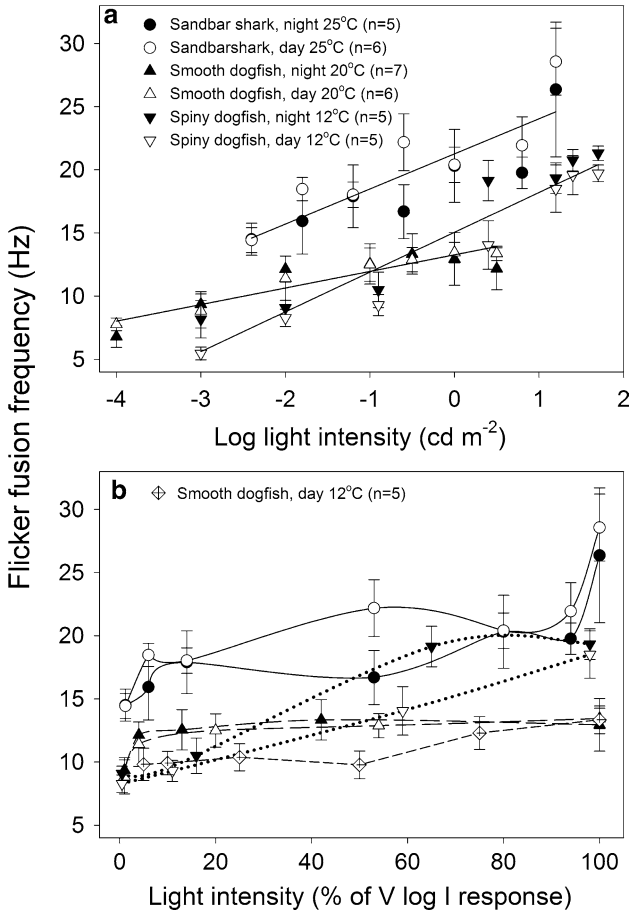

Fig. 6 Mean flicker fusion frequency (±SEM) versus light intensity in sandbar shark at 25EC (*circles*), smooth dogfish at 20 °C (*triangles*), and spiny dogfish 12 °C (*inverted triangles*), and smooth dogfish at 12 °C (*diamonds*). In all cases, *open symbols* are data from day experiments and *filled symbols* data from night experiments. **a** Light intensity is expressed in log units of cd m^{-2}. **b** Light intensity is expressed as the fractional value of that needed to produce the maximal responses in the V log I experiments shown in Fig. 5

therefore, combined within species for regression analyses of the relationship of LLI to FFF. There was a positive linear relationship between FFF and LLI for all three species (Fig. 6a):

$$\text{Sandbar shark}: \ \text{FFF} = 2.78\ \text{LLI}\ (\pm 0.47) + 21.3(\pm 0.6)\ \left(r^2 = 0.74\right) \quad (5)$$

$$\text{Smooth dogfish}: \ \text{FFF} = 1.31\ \text{LLI}\ (\pm 0.15) + 13.3(\pm 0.3)\ \left(r^2 = 0.84\right) \quad (6)$$

$$\text{Spiny dogfish}: \ \text{FFF} = 3.14\ \text{LLI}\ (\pm 0.27) + 15.1(\pm 0.5)\ \left(r^2 = 0.91\right) \quad (7)$$

(values in parentheses are SEM).

Because of the highly non-linear relationship between response amplitude and LLI (Fig. 5), however, we argue that relating FFF to LLI gives a somewhat misleading impression of the functional characteristics of the visual system. We, therefore, also graphed FFF versus light

Table 3 Mean (±SEM) flicker fusion frequency (FFF, in Hz) of sandbar shark, smooth dogfish and spiny dogfish at maximum light intensities (V_{max} = 0.8, 0.5, and 1.4 LLI, respectively), and light intensities 25 % of these values (25 % V_{max} LLI)

Species	V_{max} LLI	25 % V_{max} LLI
Sandbar shark	$21 \pm 1^{*,+}$	$17 \pm 0.9^{*}$
Smooth dogfish	$13 \pm 0.9^{\#,+}$	12 ± 0.6
Spiny dogfish	$20 \pm 0.9^{*,\#}$	$14 \pm 2^{*}$

* Significant difference between light intensities within species ($P < 0.05$)

$^{\#,+}$ Significant difference between species within light intensities ($P < 0.05$)

intensity, but with latter expressed as that required to produce a given fractional response based on the *V* log *I* curves (Fig. 5). When plotted in this way (Fig. 6b), it is apparent that FFF remains largely unchanged over the majority of the operational range of light intensities in sandbar shark and smooth dogfish. The FFF of spiny dogfish, in contrast, showed a generally increasing FFF with light intensity over their operational range of light intensities.

Although there were no significant differences in mean FFF values between species at LLI 25 % of that needed to produce V_{max}, there were significant differences between species over all pairwise comparisons at maximum light intensities (Table 3). Stimulus contrast had little to no effect on FFF in all three species at both light intensities until contrast fell well below 50 %, and in most instances not until contrast fell below 10 % (Fig. 7). The only clear exception was in spiny dogfish at the lower light intensity (i.e., LLI 25 % of that needed to produce V_{max}), where FFF diminished rapidly at contrast levels below 50 %. To provide data that are directly comparable between species, FFF experiments were also conducted on a separate group of smooth dogfish at 12 °C at LLI intensities required to produce 5, 10, 25, 50, 75, and 100 % of the maximum response. The FFF values at this lower temperature were unchanged from those at 20 °C on LLI above those required to produce *V* log *I* responses above 50 % of the maximum (Fig. 6b). Below this light level, FFFs appear only slightly reduced at the colder temperature (from ~12 Hz at 20 °C to ~10 Hz at 12 °C).

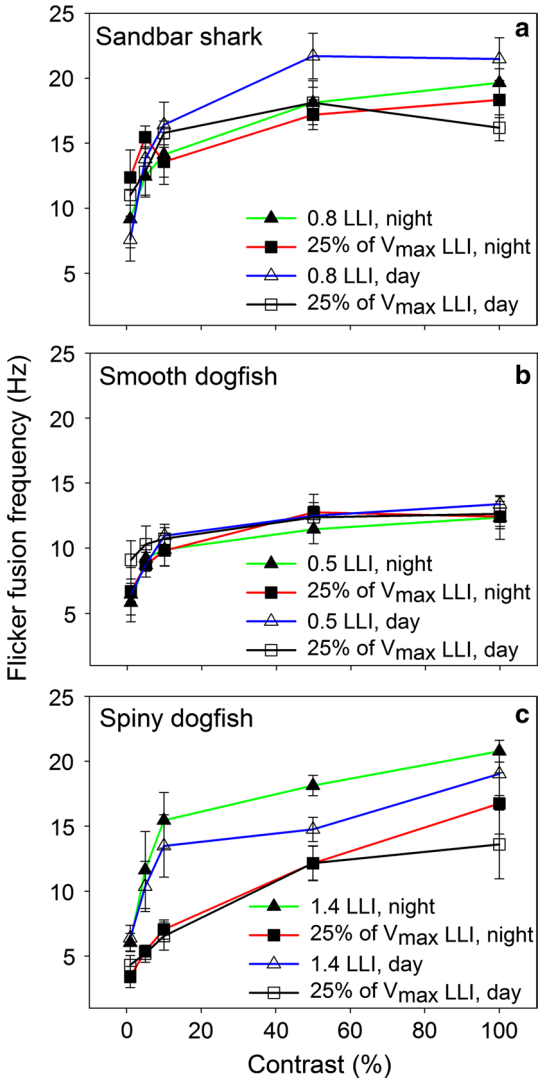

Fig. 7 Mean flicker fusion frequency (±SEM) versus contrast in sandbar shark at 25 °C (**a**), smooth dogfish at 20 °C (**b**), and spiny dogfish at 12 °C (**c**). Two light intensities were tested at each contrast step, one equal to 25 % of light intensities (*triangles*) needed to produce the maximum responses in the V log I experiments (shown in Fig. 5), and the other at 0.8, 0.5, or 1.4 LLI (*squares*) which were approximately the intensities required to produce the maximum responses. *Open symbols* are data from day experiments and *filled symbols* data from night experiments. The numbers of individuals assessed were the same as those shown in Fig. 6

Discussion

Spectral sensitivity

Light intensity and spectral composition underwater are exceedingly variable, differing both spatially (proximity to shore, depth) and temporally (daily, seasonally, or due to meteorological conditions) (McFarland 1986, 1991). Visible light decreases rapidly below 100 m even in the clearest pelagic seas, while the bandwidth becomes increasingly narrow and to center primarily on the shorter (blue) wavelengths (~480 nm) (Jerlov 1968, 1974; Lythgoe 1988; Loew and McFarland 1990). In contrast, temperate coastal seas and estuaries generally have a greenish tint (due to high concentrations of dissolved organic matter) and tend to be very turbid (due to high concentrations of phytoplankton and suspended particles). In estuaries at midday, downwelling light near the bottom has a maximum

irradiance range spanning ~570–700 nm, although during crepuscular periods this shifts to 490–520 nm (Forward et al. 1988). In coastal areas, maximal irradiance is slightly narrower and shifted to shorter wavelengths (500–570 nm) (Forward et al. 1988). High turbidity in these areas also results in rapid light attenuation with depth as well as light scattering. The former reduces overall brightness and the latter reduces the contrast of the image on the retina, and is a major factor in limiting the overall visibility (Lythgoe 1988; McFarland and Munz 1975a, b).

The spectral properties of the visual systems of sandbar shark, smooth dogfish, and spiny dogfish all appear reasonably well adapted to the light conditions in their inshore coastal habitats (Levine and MacNichol 1979; Lythgoe and Partridge 1991). The peak spectral sensitivities of the three species (470–520 nm, Fig. 2) are, however, blue-shifted compared to the green to orange wavelengths distinctive of estuaries (McFarland 1986), but are matched to the maximum irradiance range in these areas during twilight. Smooth dogfish are primarily active during crepuscular periods and at night (Casterlin and Reynolds 1979). When searching for prey during twilight hours, their peak spectral sensitivity would be matched to the photic environment and should, therefore, increase predatory success (McComb et al. 2010). There were no day–night differences in spectral sensitivity of sandbar sharks or smooth dogfish, although spiny dogfish did exhibit a Purkinje shift similar to that recorded in lemon sharks (*Negaprion brevirostris*) when going from photopic to scotopic conditions (Cohen et al. 1977). We also note, however, that the peak spectral sensitivity for smooth dogfish (478 nm) is significantly blue-shifted compared to other members of the family Triakidae: gray smoothhound (*Mustelus californicus*) (499 nm), leopard shark (*Triakis semifasciata*) (502 nm), and brown smoothhound (*Mustelus henlei*) (496 nm) (Sillman et al. 1996). Yet all are coastal bottom dwellers inhabiting waters <100 m (Crescitelli et al. 1985) and would most likely experience similar photic environments. Given that smooth dogfish are crepuscular and nocturnal forgers (Casterlin and Reynolds 1979), we hypothesize that absorbance peak of their rod pigment may instead be matched to the spectral peak (474 nm) of dinoflagellate bioluminescence from organisms such as *Pyrocystis fusiformis* (Morishita et al. 2002). Dinoflagellate-produced light has been demonstrated to facilitate cephalopod and teleost predation in darkness when prey movements induce silhouetting (Mensinger and Case 1992; Fleisher and Case 1995). Weakfish (*Cynoscion regalis*, a crepuscular–nocturnal forager) also have the most blue-shifted visual pigments of the sciaenid fishes inhabiting Chesapeake Bay investigated by Horodysky et al. (2008), and this observation likewise suggests that they too exploit the silhouetting of prey against a background of bioluminescence to enhance foraging success.

Any influence of filtering by ocular media in our ERG data would most likely be minimal due to the relatively flat transmission–wavelength curves of the cornea, lens, and vitreous of all three species (Fig. 4). Our observations agree with similar data on ocular media filtering of tissues from juvenile sandbar sharks recorded by Litherland et al. (2009). We did not, however, observe the removal of UV wavelengths by the lens tissue of spiny dogfish that these authors demonstrated in shortspine spurdog (*Squalus mitsukurii*) and which they proposed enhances the detection of bioluminescent prey. Overall, the ranges of spectral sensitivities we found are in general congruence with those of other shark species recorded using ERG (O'Gower and Mathewson 1967; Govardovskii and Lychakov 1977; Gačić et al. 2007b; McComb et al. 2010). The chromatic properties of the visual systems of sandbar shark, smooth dogfish, and spiny dogfish (Fig. 2) we measured are also generally consistent with the absorbance spectra of 17 shark species investigated using single receptor MSP by Hart et al. (2011). Based on histological and MSP analyses, Hart et al. (2006) concluded that sharks are cone monochromats and our spectral template fits (Fig. 3) for sandbar shark, smooth dogfish and spiny dogfish are congruent with this conclusion. The rhodopsin template fitting procedures (Fig. 3) we applied to our data show the expected consistency of single (presumably) rod-based shorter wavelength pigment (maximum absorptions 472–481 nm) and a single longer wavelength (presumably) cone-based pigment (maximum absorptions 520–544 nm). Because the proposed rod and cone visual pigments differ by ~47–66 nm, it is possible that sharks have some rudimentary ability to discriminate chromaticity by comparing the signals from rods and cones, in addition to luminosity sensitivity (Lythgoe and Partridge 1991). There was no evidence of any UV-absorbing pigment, with the exception of a β band on the long wavelength cone-based pigment in sandbar shark. The incomplete agreement of our results with the single receptor MSP data (rod and cone wavelengths of maximum absorbance 484–518 nm and 532–561 nm, respectively; Hart et al. 2011) may have resulted from differences in the ontogenetic state or different visual habitats of our respective subjects (Cohen 1991; Litherland 2009; Litherland et al. 2009), the generally poor performance of rhodopsin templates at short wavelengths (Govardovskii et al. 2000), or a combination of these factors.

We assert, however, that the most important feature of the spectral sensitivity curves of the three elasmobranch species we studied was their relative narrowness, especially at the longer wavelength end of the spectrum (Fig. 2), compared to the spectral sensitivity curves of sympatric inshore and estuarine teleost species from Chesapeake Bay and western north Atlantic recorded by Horodysky et al. (2008, 2010, 2013) using the same methodology. While purely

Table 4 Summary of the 50 % values from the normalized *V* log *I* curves in sympatric teleost and elasmobranch species from inshore areas of the mid-Atlantic region of the US east coast, and two US Pacific coast species. Teleost data are from Horodysky et al. (2008, 2010, 2013) and Brill et al. (2008)

Species	Day/night 50 % points from normalized *V* log *I* curves
Black rockfish (*Sebastes melanops)*	2.1/2.0
Striped bass (*Morone saxatilis*)	1.91/0.27
Bluefish (*Pomatomus saltatrix*)	1.01/0.17
Cobia (*Rachycentron canadum*)	0.97/0.58
Black sea bass (*Centropristis striata*)	0.74/0.08
Weakfish (*Cynoscion regalis*)	0.70/0.45
Spotted sea trout (*Cynoscion nebulosus*)	0.52/0.38
Red drum (*Sciaenops ocellatus*)	0.30/0.25
Spiny dogfish (*Squalus acanthias*)	0.26
Tautog (*Tautoga onitis*)	0.24/0.15
Summer flounder (*Paralichthys dentatus*)	0.14/0.17
Spot (*Leiostomus xanthurus*)	0.05/0.5
Pacific halibut (*Hippoglossus stenolepis*)	−0.09/−0.07
Atlantic croaker (*Micropogonias undulatus*)	−0.24/−0.18
Spadefish (*Chaetodipterus faber*)	−0.26/−0.10
Smooth dogfish (*Mustelus canis*)	−0.42
Sandbar shark (*Carcharhinus plumbeus*)	−0.49

conjectural, we hypothesize that the potential spectral sensitivity of sharks is limited because, unlike teleosts and for yet undescribed reasons, sharks are developmentally limited to cone monochromacy, although the peak absorbencies of the cone-based pigment have been shifted by selective pressure to match visual function to species' ecology and feeding strategies. We, therefore, posit an alternative conclusion from that of Hart et al. (2011) that cone monochromacy is "… a common strategy in the marine environment… that both sharks and marine mammals may have arrived at…by convergent evolution". Rather we suggest that it may be a limitation imposed by elasmobranch ontogeny or phylogeny, or both.

The three sympatric shark species we studied all have rod-dominated retinas, although rod-to-cone ratios differ significantly between species: smooth dogfish 100:1 (Stell and Witkovsky 1973), spiny dogfish 50:1 (Stell 1972), and sandbar shark 13:1 (Gruber et al. 1975). Hart et al. (2006) attributed rod-to-cone ratio differences in elasmobranchs primarily to habitat differences–with lower rod-to-cone ratios occurring in shallow dwelling diurnally active species, and higher rod-to-cone ratios occurring in nocturnal or deep-dwelling species. The 100:1 rod-to-cone ratio in the retina of nocturnally active smooth dogfish certainly fits this model. We suggest, however, that rod-to-cone ratios may also reflect phylogeny as well as habitat. All members of the family Carcharhinidae (which includes sandbar shark) investigated to date have rod-to-cone ratios of 13:1 or less (Table 13.2, Hart et al. 2006), even though sandbar sharks occupy the same estuarine and inshore habitats as smooth dogfish and spiny dogfish.

Luminous sensitivity and FFF

The general consensus is that shark eyes have high luminous sensitivity but with moderate to low spatial resolution, and that these characteristics result from the high convergence of photoreceptors onto ganglion cells (Gruber 1977; Bozzano and Collin 2000; Bozzano et al. 2001; Bozzano 2004; Lisney and Collin 2008; Litherland and Collin 2008) and the presence of a tapetum lucidum (Heath 1991; Braekevelt 1994; Newman et al. 2013). The structure of the tapetum lucidum of sandbar shark has been described in detail and differences noted in the reflective characteristics between populations occupying different optical environments (Litherland et al. 2009); the latter implying the critical importance of this structure to visual function. We have noted the presence of a tapetum lucidum in both spiny dogfish and smooth dogfish (unpublished observations), and this structure has been formally described in other members of the families Squalidae and Triakidae (Fishelson and Baranes 1999; Litherland et al. 2009). It is possible, therefore, that some of the differences in light sensitivity we observed between sandbar shark, smooth dogfish, and spiny dogfish were due to differences in spatial summation (i.e., differences in the convergence of photoreceptors onto ganglion cells) and to differences in the reflective properties of the tapetum lucidum, including the ability of the migration of melanosomes to occlude this structure (Litherland et al. 2009).

We suggest, however, that the differences in luminous sensitivities both between and within teleosts and elasmobranchs are also due to differences in temporal summation (i.e., integration time) which are evinced as differences in FFF (Warrant 1999, 2004). Our data on the FFF and the luminous sensitivity (i.e., the 50 % points from normalized *V* log *I* curves) of sandbar shark and smooth dogfish versus those of teleosts are consistent with this conclusion. The teleost species listed in Table 4 are all less light sensitive (i.e., have higher values for the 50 % points from normalized *V* log *I* curves) than these two elasmobranch species and all have higher maximum FFF [~40–74 Hz for the teleost species (Horodysky et al. 2008, 2010, 2013) versus ~12–29 Hz for sandbar shark and smooth dogfish] because of the reciprocal relationship of temporal summation and FFF (i.e., high temporal summation inevitably results in low FFF) (Warrant 1999, 2004). The piscivorous teleost species, striped bass (*Morone saxatilis*), bluefish (*Pomatomus saltatrix*), and cobia (*Rachycentron canadum*), that

often hunt highly mobile prey in brightly lit surface water (Bowman et al. 2000; Arendt et al. 2001; Harding and Mann 2001; Water et al. 2003), all have visual systems with a high FFF (74, 56, 65 Hz, respectively) but a low luminous sensitivity (Horodysky et al. 2010), which we argue is due (at least in part) to low temporal summation. Moreover, the littoral eurytrophic elasmobranch species, blacknose (*Carcharhinus acronotus*), scalloped hammerhead, (*Sphyrna lewini*), bonnethead (*Sphyrna tiburo*), and tiger shark (*Galeocerdo cuvie*) feed on a variety of organisms (Compagno 1990), and all have lower FFFs: 18, 27, 31, and 38 Hz, respectively (McComb et al. 2010; Litherland 2009) than striped bass, bluefish and cobia although both groups occupy a roughly equivalent trophic position. We propose that the lower FFF of these elasmobranchs likewise results from greater luminous sensitivities achieved through greater temporal summation.

We therefore posit that, in general, temporal summation in both elasmobranchs and teleosts is plastic, and that selective pressures favor greater luminous sensitivity at the expense of higher FFF in some elasmobranch species, rather than the differences in retinal function between teleosts and elasmobranchs being a result of genetically fixed anatomical or functional differences. Further support for our position comes from our observations of relatively high FFF in spiny dogfish. Their luminous sensitivity (expressed as the 50 % point of the *V* log *I* curve) is at the upper end of the teleost range (Table 4) and we hypothesize that this is a consequence of a high speed of vision (i.e., high FFF) being a requirement of their hunting and feeding strategies, and their usual occupancy of colder water temperatures than sandbar shark or smooth dogfish (Collette and Klein-MacPhee 2002; Grubbs and Musick 2007; Grubbs et al. 2007, Conrath and Musick 2008). Colder temperatures reduce FFF in teleosts generally with a Q_{10} of approximately 2 (Hanyu and Ali 1964; Ali and Muntz 1973; Fritsches et al. 2005). Therefore, if spiny dogfish are to avoid a much reduced FFF at water temperatures of 12 °C or less, this requires a lessened temporal summation with the concomitant reduction in luminous sensitivity (Table 4). Counter to this argument, however, is the very minimal effect of reduced temperature (12 vs. 20 °C) we recorded on the FFF of smooth dogfish (Fig. 6); but it is unknown if the low temperature sensitivity of FFF displayed by smooth dogfish extends to other elasmobranchs.

We also note that at least six pelagic shark and two ray species, as well as opah (*Lampris guttatus*) and multiple tuna and billfish species, have independently evolved the ability to maintain brain and retinal temperatures significantly above ambient temperature (e.g., Carey 1982; Block and Carey 1985; Block 1986; Alexander 1996; Runcie et al. 2009). Elevated retinal temperatures have, in turn, been shown to allow high FFFs at cold water temperatures without a concomitant reduction in luminous sensitivity, at least in swordfish (*Xiphias gladius*) (Fritsches et al. 2005), and presumably also do so in the other species with this adaptation. We therefore conclude, as have others (e.g., Healy et al. 2013) that this demonstrates the existence of strong selective pressure for the maintenance of adequate temporal resolution and that visual function is strongly influenced by the need to match feeding ecology to specific visual conditions even in sympatric species (e.g., Horodysky et al. 2008, 2010, 2013; McComb et al. 2013). But because spiny dogfish do not have the ability to maintain elevated retinal temperatures, the selective pressure to maintain an adequate temporal resolution (i.e., high FFF) at the colder temperatures they normally occupy requires a reduced temporal summation (and therefore a concomitant reduction in luminous sensitivity) compared to the other shark species we examined.

Sandbar shark, smooth dogfish, and spiny dogfish all show the expected linear increase in FFF with LLI (Fig. 6), as do the teleost species studied to date (e.g., Horodysky et al. 2008, 2010, 2013). We reason, however, that a more appropriate way to analyze these data is to express light levels as a fraction of the light level needed to induce maximal responses in the *V* log *I* curves (Fig. 6). Expressed in this way, it is obvious that in sandbar shark and smooth dogfish, FFF is nearly unaffected by light level over most of the dynamic operating range of these species' visual systems. In contrast, FFF in spiny dogfish increases with light intensity over the dynamic operating range of their visual system. But we argue that this observation also supports our contention that FFF is an important characteristic in spiny dogfish for matching visual system function to visual conditions and feeding/hunting strategies.

There is some information on the contrast thresholds at different frequencies in goldfish (Bilotta et al. 1998), but to the best of our knowledge we are the first to measure the effects of contrast on the FFF of any elasmobranch species. In general, FFF is unaffected by contrast, except at the lower light intensities in spiny dogfish (Fig. 7). These observations indicate that the retinas of all three shark species would be adept at tracking moving objects even when the differences in relative brightness between the objects and the background are small.

Collectively, the performances of the visual systems of the three sympatric coastal shark species (sandbar shark, smooth dogfish, and spiny dogfish) are consistent with their lifestyle and habitat use. However, their visual performance can also be placed in context of the visual performance of sympatric teleost fishes from mid-Atlantic coastal waters. Relative to performance of the visual systems of the piscivorous teleost fishes studied using the same methodology (Horodysky et al. 2010, 2013), sandbar shark and smooth dogfish have visual systems with greater luminous sensitivity but lower FFF, implying that the two shark species

achieve the former at the expense of the latter. In other words, in sandbar shark and smooth dogfish, selective pressures favor luminous sensitivity over speed of vision. Conversely, in spiny dogfish, selective pressures appear to favor the maintenance of FFFs at colder temperatures equivalent to the other two shark species through decreased temporal summation. This, in turn, necessarily results in the observed reduction in luminous sensitivity. Relative to benthic foraging teleost species from the same or similar environment studied using the same methodology (Brill et al. 2008; Horodysky et al. 2008), spiny dogfish have somewhat reduced luminous sensitivity, whereas sandbar shark and smooth dogfish have much greater luminous sensitivity. We assert that these observations support our premise that selective pressures favor luminous sensitivity over speed of vision in sandbar shark and smooth dogfish, but speed of vision over luminous sensitivity in spiny dogfish.

Acknowledgments All animal capture, care, and experimental protocols complied with relevant laws of the United States and were approved by the Institutional Animal Care and Use Committees of the College of William and Mary, Nova Southeastern University, and the University of Massachusetts Dartmouth. The authors thank the staff at the Virginia Institute of Marine Science—Eastern Shore Laboratory for their continuing hospitality and help in acquiring sandbar sharks and smooth dogfish, D. Bernal (University of Massachusetts, Dartmouth) for making it possible to perform experiments on spiny dogfish, and L. Litherland for her support and discussions regarding experimental design, execution, and data analysis. M. Kalinoski's participation was funded in part by a scholarship from the South Florida Chapter of the Explorer's Club. This paper is contribution 3409 from the Virginia Institute of Marine Science, College of William & Mary. The opinions expressed herein are those of the authors and do not necessarily reflect the views of the U.S. Department of Commerce—National Oceanic and Atmospheric Administration (NOAA) or any of its subagencies. Mention of trade names, products, or commercial companies is for identification purposes only and likewise does not imply endorsement by NOAA or any of its subagencies.

References

Able KW, Fahay MP (2010) Ecology of the estuarine fishes: temperate waters of the western North Atlantic. The John Hopkins University Press, Baltimore

Alexander RL (1996) Evidence of brain-warming in the mobulid rays, Mobula tarapacana and Manta birostris (Chondrichthyes: Elasmobranchii: Batoidea: Myliobatiformes). Zool J Linn Soc-Lond 118:151–164

Ali MA, Muntz WRA (1973) Electroretinography as a tool for studying fish vision. In: Ali MA (ed) Vision in fishes, new approaches in research. NATO advanced study institute series, vol 1. Plenum Press, New York, pp 159–167

Ali MA, Anctil M, Cervetto L (1978) Photoreception. In: Ali MA (ed) Sensory ecology, review and perspectives. Plenum Press, New York, pp 467–502

Arendt MD, Olney JE, Lucy JA (2001) Stomach content analysis of cobia, *Rachycentron canadum*, from lower Chesapeake Bay. Fish Bull 99:665–670

Armington JC (1974) The Electroretinogram. Academic Press, New York

Bedore CN, Ellis R, Loew ER, Frank TM, Hueter RE, McComb DM, Kajiura SM (2013) A physiological analysis of color vision in batoid elasmobranchs. J Comp Physiol A 199:1129–1141

Bilotta J, Lynd FM, Powers MK (1998) Effects of mean luminance on goldfish temporal contrast sensitivity. Vis Res 38:55–59

Bleckmann H, Hofmann MH (1999) Special senses. In: Hamlett WC (ed) Sharks, skates, and rays: the biology of elasmobranch fishes. The Johns Hopkins University Press, Baltimore, pp 300–308

Block BA (1986) Structure of the brain and eye heater tissue in marlins, sailfish and spearfish. J Morphol 190:169–189

Block BA, Carey FG (1985) Warm brain and eye temperatures in sharks. J Comp Physiol B 156:229–236

Bowman RW, Stillwell CE, Michaels WL, Grosslein MD (2000) Food of northwest Atlantic fishes and two common species of squid. NOAA Technical Memorandum NMFS-NE-155. Northeast Region, Northeast Fisheries Science Center, Woods Hole, p 137

Bozzano A (2004) Retinal specializations in the dogfish *Centroscymnus coelolepis* from the Mediterranean deep-sea. Sci Mar 68(Suppl 3):185–195

Bozzano A, Collin SP (2000) Retinal ganglion cell topography in elasmobranchs. Brain Behav Evol 55:191–208

Bozzano A, Murgia R, Vallerga S, Hirano J, Archer S (2001) The photoreceptor system in the retinae of two dogfishes, *Scyliorhinus canicula* and *Galeus melastomus*: possible relationship with depth distribution and predatory lifestyle. J Fish Biol 50:1258–1278

Braekevelt CR (1994) Fine structure of the choroidal tapetum lucidum in the Port Jackson shark (*Heterodontus phillipi*). Anat Embryol (Berl) 190:591–596

Brill R, Magel C, Davis M, Hannah R, Rankin P (2008) Effects of rapid decompression and exposure to bright light on visual function in black rockfish (*Sebastes melanops*) and Pacific halibut (*Hippoglossus stenolepis*). Fish Bull 106:427–437

Brown KT (1968) The electroretinogram: its components and their origins. Vis Res 8:633–677

Bullock TH, Hofmann MH, New JG, Nahm FK (1991) Dynamic properties of visual evoked potentials in the tectum of cartilaginous and bony fishes, with neuroethological implications. J Exp Zool 256(Suppl 5):142–155

Burnham KP, Anderson DR (2002) Model selection and multimodel inference: a practical information-theoretic approach. Springer, New York

Carey FG (1982) A brain heater in the swordfish. Science 216:1327–1329

Casterlin ME, Reynolds WW (1979) Diel activity patterns of the smooth dogfish shark, *Mustelus canis*. Bull Mar Sci 29:440–442

Coates MM, Garm A, Theobald JC, Thompson SH, Nilsson DE (2006) The spectral sensitivity of the lens eyes of a box jellyfish, *Tripedalia cystophora*. J Exp Biol 209:3758–3765

Cohen JL (1991) Adapation for scotopic vision in the lemon shark (*Negaprion brevirostris*). J Exp Zool 5:76–84

Cohen JL, Gruber SH, Hamasaki DI (1977) Spectral sensitivity and purkinje shift in the retina of the lemon shark, *Negaprion brevirostris* (Poey). Vis Res 17:787–792

Collette BB, Klein-MacPhee G (2002) Bigelow and Schroeder's Fishes of the Gulf of Maine, 3rd edn. Smithsonian Institution Press, Washington, DC

Compagno LJV (1984a) FAO Species Catalogue. Vol. 4. Sharks of the world: an annotated and illustrated catalogue of shark species known to date, Part 1 Hexanchiformes to Lamniformes. FAO Fish Synop 4(1):1–249

Compagno LJV (1984b) FAO Species Catalogue. Vol. 4. Sharks of the world: an annotated and illustrated catalogue of shark species known to date, Part 2 Carcharhiniformes. FAO Fish Synop 4(2):251–655

Compagno LJV (1990) Alternative live-history styles of cartilaginous fishes in time and space. Environ Biol Fishes 28:33–75
Compagno LJV (2003) Sharks of the order Carcharhiniformes. Blackburn Press, New Jersey
Conrath CL, Musick JA (2002) Reproductive biology of the smooth dogfish, *Mustelus canis*, in the northwest Atlantic Ocean. Environ Biol Fishes 64:367–377
Conrath CL, Musick JA (2008) Investigations into depth and temperature habitat utilization and overwintering grounds of juvenile sandbar sharks, *Carcharhinus plumbeus*: the importance of near shore North Carolina waters. Environ Biol Fish 82:123–131
Crescitelli F, McFall-Ngai M, Horwitz J (1985) The visual pigment sensitivity hypothesis: further evidence from fishes of varying habitats. J Comp Physiol A 157:323–333
Douglas RH (2001) The ecology of teleost fish visual pigments: a good example of sensory adaptation to the environment? In: Schmid A (ed) Ecology of Sensing. Springer, Berlin, pp 215–235
Evans LS, Peachy NS, Marchese AL (1993) Comparison of three methods of estimating the parameters of the Naka-Rushton equation. Doc Ophthalmol 84:19–30
Fishelson L, Baranes A (1999) Ocular development in the oman shark, *Iago omanensis* (Triakidae), Gulf of Aqaba, Red Sea. Anat Rec 256:389–402
Fleisher KJ, Case JF (1995) Cephalopod predation facilitate by dinoflagellate luminescence. Biol Bull 189:263–271
Forward RB, Cronin TW, Douglas JK (1988) The visual pigments of carbs. II. Environmental adaptations. J Comp Physiol 162A:479–490
Frank TM (1999) Comparative study of temporal resolution in the visual systems of mesopelagic crustaceans. Biol Bull 196:137–144
Frank TM (2000) Temporal resolution in mesopelagic crustaceans. Philos Trans R Soc 355:1195–1198
Frank TM (2003) Effects of light adaptation on the temporal resolution of deep-sea crustaceans. Integr Comp Biol 43:559–570
Fritsches KA, Brill RW, Warrant EJ (2005) Warm eyes provide superior vision in swordfishes. Curr Biol 15:55–58
Gačić Z, Damjanovic I, Bajic A, Milosevic M, Mickovic B, Nikcevic M, Andjus PR (2007a) The d-wave in fish and the state of light adaptation. Gen Physiol Biophys 26:260–267
Gačić Z, Damjanović I, Mićković B, Hegedič A, Nikčević M (2007b) Spectral sensitivity of the dogfish shark *Scyliorhinus canicula*. Fish Physiol Biochem 33:21–27
Gelsleichter J, Musick JA, Nichols S (1999) Food habits of the smooth dogfish, *Mustelus canis*, dusky shark, *Carcharhinus obscurus*, Atlantic sharpnose shark, *Rhizoprionodon terraenovae*, and the sand tiger, *Carcharias taurus*, from the northwest Atlantic Ocean. Environ Biol Fishes 54:205–217
Govardovskii VI, Lychakov LV (1977) Visual cells and visual pigments in the Black Sea elasmobranchs. Zh Evol Biokhim Fiziol 13:162–166
Govardovskii VI, Fyhrquist N, Reuter T, Kuzmin DG, Donner K (2000) In search of the visual pigment template. Vis Neurosci 17:509–528
Grubbs RD, Musick JA (2007) Spatial delineation of summer nursery areas for juvenile sandbar sharks in Chesapeake Bay, Virginia. Am Fish Soc Symp 50:63–86
Grubbs RD, Musick JA, Conrath CL, Romaine JG (2007) Long-term movements, migration, and temporal delineation of summer nurseries for juvenile sandbar sharks in the Chesapeake Bay region. Am Fish Soc Symp 50:87–108
Gruber SH (1977) The visual system of sharks: adaptations and capability. Am Zool 17:453–469
Gruber SH, Gulley RL, Brandon J (1975) Duplex retina in seven elasmobranch species. Bull Mar Sci 25:353–358
Hamasaki DI, Bridges CDB (1965) Properties of the electroretinogram in three elasmobranch species. Vis Res 5:483–496
Hamasaki DI, Bridges CDB, Meneghini KA (1967) The electroretinogram of three species of elasmobranchs. In: Gilbert PW, Mathewson RF, Rall DP (eds) Sharks. skates, and rays. The Johns Hopkins Press, Baltimore, pp 447–463
Hanyu I, Ali MA (1964) Electroretinogram and its flicker fusion frequency at different temperatures in light-adapted salmon (*Salmo salar*). J Cell Comp Physiol 63:309–322
Harding JM, Mann R (2001) Diet and habitat use by bluefish, *Pomatomus saltatrix*, in a Chesapeake Bay estuary. Environ Biol Fish 60:401–409
Hart NS, Lisney TJ, Marshall NJ, Collin SP (2004) Multiple cone visual pigments and the potential for trichromatic colour vision in two species of elasmobranch. J Exp Biol 207:4587–4594
Hart NS, Lisney TJ, Collin SP (2006) Visual communication in elasmobranchs. In: Kapoor BG, Ladich F, Collin SP, Raschi WG (eds) Fish communication, vol 2. Science Publishers Inc., Enfield, pp 337–392
Hart NS, Theiss SM, Harahush BK, Collin SP (2011) Microspectrophotometric evidence for cone monochromacy in sharks. Naturwissenschaften 98:193–201
Healy K, McNally L, Ruxton GD, Cooper N, Jackson AL (2013) Metabolic rate and body size are linked with perception of temporal information. Anim Behav 86:685–696
Heath AR (1991) The ocular tapetum lucidum: a model system for interdisciplinary studies in elasmobranch biology. J Exp Zool 256(Suppl S5):41–45
Hodgson ES, Mathewson RF (1978) Sensory biology of sharks, skates, and rays. Government Printing Office, Washington, DC
Horodysky AZ, Brill RW, Warrant EJ, Musick JA, Latour RJ (2008) Comparative visual function in five sciaenid fishes inhabiting Chesapeake Bay. J Exp Biol 211:3601–3612
Horodysky AZ, Brill RW, Warrant EJ, Musick JA, Latour RJ (2010) Comparative visual function in four piscivorous fishes inhabiting Chesapeake Bay. J Exp Biol 213:1751–1761
Horodysky AZ, Brill RW, Crawford KC, Seagroves ES, Johnson AK (2013) Comparative visual ecophysiology of mid-Atlantic temperate reef fishes. Biol Open 2:1371–1381
Hueter RE (1991) Adaptations for spatial vision in sharks. J Exp Zool Suppl 5:130–141
Hueter RE, Mann DA, Maruska KP, Sisneros JA, Semski LS (2004) Sensory biology of elasmobranchs. In: Carrier JC, Musick JA, Heithaus MR (eds) Biology of sharks and their relatives. CRC Press, Boca Raton, pp 325–368
Jerlov NG (1968) Optical oceanography. Elsevier, Amsterdam
Jerlov NG (1974) Optical aspects of oceanography. Academic Press, London
Johnson ML, Shelton PMJ, Gaten E (2000) Temporal resolution in the eyes of marine decapods from coastal and deep-sea habitats. Mar Biol 136:243–248
Kajiura SJ (2010) Pupil dilation and visual field in the piked dogfish, *Squalus acanthias*. Enviorn Biol Fish 88:133–141
Kajiura SJ, Tallack SML (2009) Pupil dilation in the spiny dogfish. Bull Mt Desert Biol Lab 48:68
Klimley PA (2013) The Biology of sharks and rays. The University of Chicago Press, Chicago
Kobayashi H (1962) A comparative study on electroretinogram in fish, with special reference to ecological aspects. Contribution of the Shimonoseki College of Fisheries, No 253:171–248
Levine JS, MacNichol EF Jr (1979) Visual pigments in teleost fishes: effects of habitat, microhabitat, and behavior on visual system evolution. Sens Process 3:95–131
Lisney TJ, Collin SP (2008) Retinal ganglion cell distribution and spatial resolving power in elasmobranchs. Brain Behav Evol 72:59–77
Lisney TJ, Theiss SM, Collin SP, Hart NS (2012) Vision in elasmobranchs and their relatives: 21st century advances. J Fish Biol 80:2024–2054

Litherland, LE (2009) Neuroethological studies in shark vision. Ph.D. Dissertation, University of Queensland, Sensory Neurobiology Group, School of Biomedical Sciences, Brisbane, Australia, pp 211

Litherland L, Collin SP (2008) Comparative visual function in elasmobranchs: spatial arrangement and ecological correlates of photoreceptor and ganglion cell distributions. Vis Neurosci 25:549–561

Litherland L, Collin SP, Fritsches KA (2009) Visual optics and ecomorphology of the growing shark eye: a comparison between deep and shallow water species. J Exp Biol 212:3583–3594

Loew ER, McFarland WN (1990) The underwater visual environment. In: Douglas RH, Djamgoz MBA (eds) The visual system of fish. Chapman and Hall, London, pp 3–43

Losey GS, McFarland WN, Loew ER, Zamzow JP, Nelson PA, Marshall NJ (2003) Visual biology of Hawaiian coral reef fishes. I. Ocular transmission and visual pigments. Copeia 2003:433–454

Lythgoe JN (1979) The ecology of vision. Clarendon Press, Oxford

Lythgoe JN (1978) Fishes: vision in dim light and surrogate senses. In: Ali MA (ed) Sensory ecology, review and perspectives. Plenum Press, New York, pp 155–168

Lythgoe JN (1988) Light and vision in the aquatic environment. In: Atema J, Fay RR, Popper AN, Tavolga WN (eds) Sensory biology of aquatic animals. Springer, New York, pp 57–82

Lythgoe JN, Partridge JC (1991) The modelling of optimal visual pigments of dichromatic teleosts in green coastal waters. Vis Res 31:361–371

Marshall JN, Cronin TW, Frank TM (2003) Visual adaptations in crustaceans: chromatic, developmental, and temporal aspects. In: Collin SP, Marshall JN (eds) Sensory processing in aquatic environments. Springer, New York, pp 343–372

McCandless CT, Pratt HL Jr, Kohler NE, Merson RR, Recksiek CW (2007) Distributions, localized abundance, movements and migrations of juvenile sandbar sharks tagged in Delaware Bay. Am Fish Soc Symp 50:45–62

McComb DM, Frank TM, Hueter RE, Kajiura SM (2010) Temporal resolution and spectral sensitivity of the visual system of three coastal shark species from different light environments. Physiol Biochem Zool 83:299–307

McComb DM, Kajiura SM, Horodysky AZ, Frank TM (2013) Comparative visual function in predatory fishes from the Indian River lagoon. Physiol Biochem Zool 86:285–297

McFarland WN (1986) Light in the sea-correlations with behaviors of fishes and invertebrates. Am Zool 26:389–401

McFarland W (1991) Light in the sea: the optical world of elasmobranchs. J Exp Zool Suppl 5:3–12

McFarland WN, Munz FW (1975a) Part II: the photic environment of clear tropical seas during the day. Vis Res 15:1063–1070

McFarland WN, Munz FW (1975b) Part III: the evolution of photopic visual pigments in fishes. Vis Res 15:1071–1080

McMillan DG, Morse WW (1999) Essential fish habitat source document: Spiny dogfish, *Squalus acanthias*, life history and habitat characteristics. NOAA Tech Memo NMFS-NE-150, Northeast Region, Northeast Fisheries Science Center, Woods Hole, pp 19

Mensinger AF, Case JF (1992) Dinoflagellate luminescence increases susceptibility of zooplankton to teleost predation. Mar Biol 112:207–210

Morishita H, Ohashi S, Oku T, Nakajima Y, Lokima S, Ryufuku M, Nakamura H, Ohmiya Y (2002) Cloning and characterization of an active fragment of luciferase from a luminescent marine alga, *Pyrocystis lunula*. Photochem Photobiol 75:311–315

Naka KI, Rushton WAH (1966) S-potentials from luminosity units in the retina of fish (Cyprinidae). J Physiol 185:587–599

Newman AS, Marshall JN, Collin SP (2013) Visual eyes: a quantitative analysis of the photoreceptor layer in deep-sea sharks. Brain Behav Evol 82:237–249

O'Gower AK, Mathewson RF (1967) Spectral sensitivity and flicker fusion frequency of the lemon shark, *Negaprion brevirostris*. In: Gilbert PW, Mathewson RF, Rall DP (eds) Sharks, skates, and rays. The Johns Hopkins Press, Baltimore, pp 433–446

R Development Core Team (2008) R: a language and environment for statistical computing. R Foundation for Statistical Computing, Vienna

Ross LG, Ross B (1999) Anesthetic and sedative techniques for aquatic animals. Blackwell Science Ltd., Oxford

Rountree RA, Able KW (1996) Seasonal abundance, growth, and foraging habits of juvenile smooth dogfish, *Mustelus canis*, in a New Jersey estuary. Fish Bull 94:522–534

Runcie RM, Dewar H, Hawn DR, Frank LR, Dickson KA (2009) Evidence for cranial endothermy in the opah (*Lampris guttatus*). J Exp Biol 212:461–470

Schieber NL, Collin SP, Hart NS (2012) Comparative retinal anatomy in four species of elasmobranch. J Morphol 273:423–440

Severns ML, Johnson MA (1993) The care and fitting of the Naka-Rushton functions to electroretinographic intensity data. Doc Ophthalmol 85:135–150

Siebeck UE, Marshall NJ (2001) Ocular media transmission in coral reef fish—can coral reef fish see ultraviolet light? Vis Res 41:133–149

Sillman AJ, Letsinger GA, Patel S, Loew ER, Klimley AP (1996) Visual pigments and photoreceptors in two species of shark, *Triakis semifasciata* and *Mustelus henlei*. J Exp Zool 276:1–10

Sloman KA, Wilson RW (2006) Anthropogenic impacts upon behavior and physiology. In: Sloman KA, Wilson RW, Balshine S (eds) Fish Physiology, Behavior and physiology of fish, vol 24. Elsevier, Amsterdam, pp 413–468

Stavenga DG, Smiths RP, Hoenders BJ (1993) Simple exponential functions describing the absorbance bands of visual pigment spectra. Vis Res 33:1011–1017

Stell WK (1972) The structure and morphologic relations of rods and cones in the retina of the spiny dogfish *Squalus*. Comp Biochem Physiol 42:141–152

Stell WK, Witkovsky P (1973) Retinal structure in the smooth dogfish, *Mustelus canis*: light microscopy of photoreceptor and horizontal cells. J Comp Neurol 148:33–46

Stillwell CE, Kohler NE (1993) Food habits of the sandbar shark *Carcharhinus plumbeus* off the U.S. northeast coast, with estimates of daily ration. Fish Bull 91:138–150

Thorpe A, Douglas RH, Truscott RJW (1993) Spectral transmission and short-wave absorbing pigments in the fish lens. I. Phylogenetic distribution and identity. Vis Res 33:289–300

Warrant EJ (1999) Seeing better at night: life style, eye design and the optimum strategy of spatial and temporal summation. Vis Res 39:1611–1630

Warrant E (2004) Vision in the dimmest habitats on earth. J Comp Physiol A 190:765–789

Water JF, Overton AS, Ferry KH, Mather ME (2003) Atlantic coast feeding habits of striped bass: a synthesis supporting a coast-wide understanding of trophic biology. Fish Manag Ecol 10:349–360

Weissburg MJ, Browman HI (2005) Sensory biology: linking the internal and external ecologies of marine organisms. Mar Ecol Prog Ser 287:263–307